MPI-PhT/95-94
October 1995

Moment analysis of energy spectra and the effect of running coupling*

Sergio Lupia†

Max-Planck-Institut für Physik, Werner-Heisenberg-Institut
Föhringer Ring 6, D–80805 München, Germany

Abstract

Single particle inclusive energy spectra in e^+e^- annihilation are analyzed in terms of moments. By assuming Local Parton Hadron Duality (LPHD), experimental data in a wide c.m. energy range from 3 GeV up to LEP energy are compared to the theoretical predictions of Modified Leading Log Approximation (MLLA) of QCD with and without taking into account the running of α_s. MLLA with running coupling (Limiting Spectrum) is found to reproduce experimental results very well, while the model with fixed coupling is inconsistent with data. Rescaled cumulants are shown to be sensitive to the running of α_s in the asymptotic regime, while the Lorentz-invariant distribution, Edn/d^3p, points out this effect at very small energy E of few hundreds MeV. These results give a direct evidence of the running of the QCD coupling in inclusive energy spectra and lend further support to the LPHD picture.

*to be published in the Proceedings of the XXVth International Symposium on Multiparticle Dynamics, Stará Lesná, Slovakia, September 12-16, 1995, Eds. D. Brunsko, L. Sandor, J. Urban, World Scientific, Singapore

†E-mail address: lupia@mppmu.mpg.de

MOMENT ANALYSIS OF ENERGY SPECTRA AND THE EFFECT OF RUNNING COUPLING

SERGIO LUPIA
Max-Planck-Institut für Physik, Werner-Heisenberg-Institut
Föhringer Ring 6, D-80805 München, Germany
E-mail: lupia@mppmu.mpg.de

ABSTRACT

Single particle inclusive energy spectra in e^+e^- annihilation are analyzed in terms of moments. By assuming Local Parton Hadron Duality (LPHD), experimental data in a wide c.m. energy range from 3 GeV up to LEP energy are compared to the theoretical predictions of Modified Leading Log Approximation (MLLA) of QCD with and without taking into account the running of α_s. MLLA with running coupling (Limiting Spectrum) is found to reproduce experimental results very well, while the model with fixed coupling is inconsistent with data. Rescaled cumulants are shown to be sensitive to the running of α_s in the asymptotic regime, while the Lorentz-invariant distribution, Edn/d^3p, points out this effect at very small energy E of few hundreds MeV. These results give a direct evidence of the running of the QCD coupling in inclusive energy spectra and lend further support to the LPHD picture.

1. Introduction

The main open problem in strong interaction phenomenology is the understanding of the hadronization mechanism. There is indeed a gap between theoretical predictions coming from perturbative QCD at parton level and experimental results at final particle level. A bridge between these two sides is given by a soft confinement mechanism[1,2]: single particle inclusive spectra are simply required to be proportional to single parton inclusive spectra obtained from perturbative QCD, provided the parton cascade is evolved down to a cutoff scale of the order of the hadronic masses $Q_0 \simeq m_h$. This hypothesis of Local Parton Hadron Duality (LPHD)[3] has been particularly successful in describing both the shape and the position of the maximum of single inclusive charged particle momentum spectra in hadronic jets in e^+e^- annihilation ranging from PETRA/PEP[4] to LEP energy[5,6,7,8]. Recently, similar results have been obtained in DIS for inclusive momentum spectra in the Breit frame at HERA[9,10].

In this paper, I report on the results obtained in collaboration with Wolfgang Ochs[11]. We performed the analysis of moments up to order 4 of single particle inclusive energy spectra in hadronic jets in e^+e^- annihilation. Since moments are sensitive to the tail of the distribution, i.e., to the low energy region, a consistent kinematical scheme has been defined to relate parton and hadron spectra. Our aim was two-fold:

firstly, to investigate the sensitivity of single particle energy spectra to the running of the coupling α_s, in particular for soft particles in the low energy region, where the coupling is stronger; secondly, to test the validity of the description in terms of perturbative QCD plus LPHD in the small c.m. energy domain.

2. The theoretical framework

2.1. MLLA Evolution Equations

The evolution equation of single parton inclusive energy distribution in the framework of MLLA is given by[2]:

$$\frac{d}{d\log\Theta}x\bar{D}_A^B(x,\log P\Theta)=\sum_{C=q,\bar{q},g}\int_0^1 dz\frac{\alpha_s(k_t)}{2\pi}\Phi_A^C(z)\left[\frac{x}{z}\bar{D}_C^B\left(\frac{x}{z},\log(zP\Theta)\right)\right] \qquad (1)$$

with the boundary condition at threshold $P\Theta = Q_0$, $x\bar{D}_A^B(x,\log Q_0)=\delta(1-x)\delta_A^B$. Here P and Θ denote the primary parton energy and jet opening angle respectively, x is the energy fraction carried by the produced parton, $\Phi_i^j(z)$ are the parton splitting kernels and i,j, A, B, C label quarks, antiquarks and gluons. The QCD running coupling is given by its one-loop expression $\alpha_s(k_t)=2\pi/b\log(k_t/\Lambda)$ with $b\equiv(11N_c-2n_f)/3$, Λ the QCD-scale and N_c and n_f the number of colors and of flavors respectively. The scale of the coupling is given by the transverse momentum $k_t\simeq z(1-z)P\Theta$. The shower evolution is cut off by Q_0, such that $k_t\geq Q_0$.

The integral equation can be solved by Mellin transform:

$$D_\omega(Y,\lambda)=\int_0^1\frac{dx}{x}x^\omega[x\bar{D}(x,Y,\lambda)]=\int_0^Y d\xi e^{-\xi\omega}D(\xi,Y,\lambda) \qquad (2)$$

with $Y=\log\frac{P\Theta}{Q_0}\simeq\log\frac{P}{Q_0}$, $\lambda=\log\frac{Q_0}{\Lambda}$, $\xi=\log\frac{P}{k}$ and parton energy k.

In flavor space the valence quark and ($\pm$) mixtures of sea quarks and gluons evolve independently with different "eigenfrequencies". At high energies, the dominant contribution to the inclusive spectrum comes from the "plus"-term, which we denote by $D_\omega(Y,\lambda)\equiv D_\omega^+(Y,\lambda)$. By keeping now, as usual, only the leading singularity in ω-space plus a constant term, one gets:

$$\left(\omega+\frac{d}{dY}\right)\frac{d}{dY}D_\omega(Y,\lambda)-4N_c\frac{\alpha_s(Y+\lambda)}{2\pi}D_\omega(Y,\lambda)=-a\left(\omega+\frac{d}{dY}\right)\frac{\alpha_s(Y+\lambda)}{2\pi}D_\omega(Y,\lambda) \qquad (3)$$

where $a=11N_c/3+2n_f/3N_c^2$ accounts for recoil effects.

By defining the anomalous dimension γ_ω according to:

$$D_\omega(Y,\lambda)=D_\omega(Y_0,\lambda)\exp\left(\int_{Y_0}^Y dy\gamma_\omega[\alpha_s(y+\lambda)]\right) \qquad (4)$$

the evolution equation for the inclusive spectrum can also be written as a differential equation for γ_ω. In general this nonlinear equation has two roots and the solution consists of a superposition of two terms of the type (4). The explicit solution of eq. (3) can be expressed indeed as a linear superposition of two hypergeometric distributions[2]. An interesting case of the general solution is the Limiting Spectrum, where the two parameters coincide, $Q_0 = \Lambda$, i.e., $\lambda = 0$. In this case, the expressions simplify and a simpler integral representation of the spectrum has been achieved.

2.2. MLLA with fixed α_s

In order to study the sensitivity of the single particle inclusive energy distribution to the running of the coupling, we built a new model based on MLLA formalism but with the coupling kept fixed at a given value. In this case, the value of the coupling or, equivalently, the value of the parameter γ_0, $\gamma_0^2 = 6\alpha_s/\pi$, replaces Λ as a free parameter of the model. Accordingly, eq. (3) becomes now:

$$\left(\omega + \frac{d}{dY}\right)\frac{d}{dY}D_\omega(Y,\lambda) - \gamma_0^2 D_\omega(Y,\lambda) = -2\eta\left(\omega + \frac{d}{dY}\right)D_\omega(Y,\lambda) \tag{5}$$

with $\eta = a\gamma_0^2/8N_c = a\alpha_s/4\pi$.

One can then perform explicitly the inverse Mellin transform and get an explicit solution for the inclusive energy spectrum in MLLA with fixed-α_s:

$$D_{fix}(\xi,Y,\lambda) = \gamma_0\sqrt{\frac{Y-\xi}{\xi}}I_1\Big(2\gamma_0\sqrt{\xi(Y-\xi)}\Big)e^{-2\eta(Y-\xi)} \tag{6}$$

3. Moment analysis: from momentum spectra to energy spectra

3.1. Moment analysis

In addition to the standard study of single particle inclusive distribution, one can also study the multiplicity $\bar{\mathcal{N}}$ and the normalized moments of the distribution, $< \xi^q(Y,\lambda) >$, given by:

$$\begin{aligned} \bar{\mathcal{N}} &= \int d\xi D(\xi,Y,\lambda) \\ < \xi^q(Y,\lambda) > &= \frac{1}{\bar{\mathcal{N}}}\int d\xi \xi^q D(\xi,Y,\lambda) \end{aligned} \tag{7}$$

or the cumulant moments $\kappa_q(Y,\lambda)$[12,13]; the latter are related to ordinary moments by a standard cluster expansion:

$$\begin{aligned} \kappa_1 &= < \xi >= \bar{\xi} \quad , \quad \kappa_2 \equiv \sigma^2 =< (\xi-\bar{\xi})^2 > \\ \kappa_3 &= < (\xi-\bar{\xi})^3 > \quad , \quad \kappa_4 =< (\xi-\bar{\xi})^4 > -3\sigma^4 \end{aligned} \tag{8}$$

One also introduces the reduced cumulants $k_q \equiv \kappa_q/\sigma^q$, in particular the skewness $s = k_3$ and the kurtosis $k = k_4$. The cumulants κ_q can be derived from the expansion:

$$\log D_\omega(Y,\lambda) = \sum_{q=0}^{\infty} \kappa_q(Y,\lambda)\frac{(-\omega)^q}{q!} \;\Leftrightarrow\; \kappa_q(Y,\lambda) = \left(-\frac{\partial}{\partial\omega}\right)^q \log D_\omega(Y,\lambda)\Big|_{\omega=0}, \quad (9)$$

with $\bar{\mathcal{N}}_E(Y,\lambda) = D_\omega(Y,\lambda)|_{\omega=0}$.

At high energies, one term of the form (4) dominates and one obtains

$$\kappa_q(Y) = \kappa_q(Y_0) + \int_{Y_0}^{Y} dy \left(-\frac{\partial}{\partial\omega}\right)^q \gamma_\omega[\alpha_s(y)]\Big|_{\omega=0} \quad (10)$$

This equation shows the direct dependence of the moments on $\alpha_s(Y)$. For fixed α_s, for example, one obtains directly $\kappa_q(Y) \propto Y$ for high energies.

Let us stress that the study of moments and cumulants is worth to be pursued, since explicit analytical expressions for their dependence on c.m. energy have been obtained[13]; moments of order q in the MLLA model with running coupling can indeed be expressed as a function of a, b, $Y+\lambda$ and λ, while moments for the Limiting Spectrum can be expressed in a simpler way in terms of the parameter $B \equiv a/b$ and the variable $z \equiv \sqrt{16N_cY/b}$. In the fixed α_s model, the solution is straightforward, since in this case the evolution equation for the anomalous dimension reduces to an algebraic equation. In addition, if the higher order cumulants ($q > 2$) are sufficiently small, one can reconstruct the ξ-distribution from the first four order cumulants, using a Distorted Gaussian parametrization of the spectrum[12].

However, let us notice again that high order moments are sensitive to the tail of the distribution; therefore, one has to look carefully at the treatment of the low energy region $E \to Q_0$. This point is discussed in detail in the next Subsection.

3.2. The rescaling procedure

In theoretical calculations, partons are taken as massless, $E_p = p_p$, but a p_t cutoff Q_0, $p_t \geq Q_0$, is needed for infrared regularization; therefore, $E_p \geq Q_0$ and the theoretical spectrum goes linearly to 0 for $E \to Q_0$. These predictions are usually compared to experimental results on single particle inclusive momentum spectrum, which show a finite tail down to very low momentum (large ξ). The difference of the two spectra in their tails could affect significantly the moment analysis. In order to cure this anomaly, let us remind that observable hadrons are massive, therefore $E_h \geq m_h$. It has been therefore suggested to identify the cutoff parameter Q_0 appearing in theoretical calculations with an effective hadron mass averaged over all charged particles. In addition, one has to look at energy spectra rather than at momentum spectra. Let us also remind that the Lorentz-invariant distribution $E\frac{dn}{d^3p}$ approximately follows an exponential law in low-energy experiments for sufficiently small energies:

$$E\frac{dn}{d^3p} \sim e^{-E/E_0} \quad (11)$$

with $E_0 \simeq 150$ MeV[14,15,16]. By performing a suitable rescaling, the spectrum $E_h dn/dp_h$ goes then linearly to 0 for $E \to Q_0$.

In conclusion, we propose to compare theoretical predictions for single particle inclusive energy spectra with the experimental spectrum

$$E_h \frac{dn(\xi_E)}{dp_h} \quad \text{vs.} \quad \xi_E = \log \frac{1}{x_E} = \log \frac{P}{E} \tag{12}$$

where an effective mass Q_0 is assigned to all particles, i.e., $E_h = \sqrt{p_h^2 + Q_0^2}$. Notice then that experimental spectra do depend on the chosen value of Q_0.

4. Results

4.1. Moments

Figure 1 shows (the logarithm of) the average multiplicity $\bar{\mathcal{N}}_E$ and the first four cumulants of charged particle energy spectra as a function of $Y = \log(\sqrt{s}/2Q_0)$ for $Q_0 = 270$ MeV. For the calculation of moments, an additional value for the bin in the unmeasured interval near $\xi_E \simeq Y$ (small momenta) has been added by linear extrapolation. Errors of the moments are taken as the sum of statistical and systematic errors. The latter particularly affects the overall normalization and then the average multiplicity; higher order moments are on the contrary independent of the overall normalization. The errors of the moments also includes the errors on the central values of ξ_E in each bin, taken as half the bin-size. The value of Q_0 has been obtained by comparing the moments determined for a selected Q_0 with the theoretical predictions of MLLA with running α_s at different values of Λ. The best agreement is obtained for the Limiting Spectrum

$$Q_0 = \Lambda \simeq 270 \pm 20 \text{ MeV} \tag{13}$$

Predictions of the Limiting Spectrum with this value of Q_0 and number of flavors $n_f = 3$ are shown in the Figure (solid lines). For the average multiplicity we added two new free parameters:

$$\bar{\mathcal{N}}_E = c_1 \frac{4}{9} 2\bar{\mathcal{N}}_{LS} + c_2 \tag{14}$$

where the factor 4/9 is the proportionality factor between quark and gluon jets and the factor 2 accounts for the two hemispheres; the two additional free parameters c_1 and c_2 give the proportionality factor between parton and hadron spectra and the leading particle contribution respectively. This second parameter is needed to recover the right behavior near threshold, as the prediction of the Limiting Spectrum does not fulfill the correct boundary conditions. The values of the two parameters have been fixed by fitting the lowest and the highest energy data points.

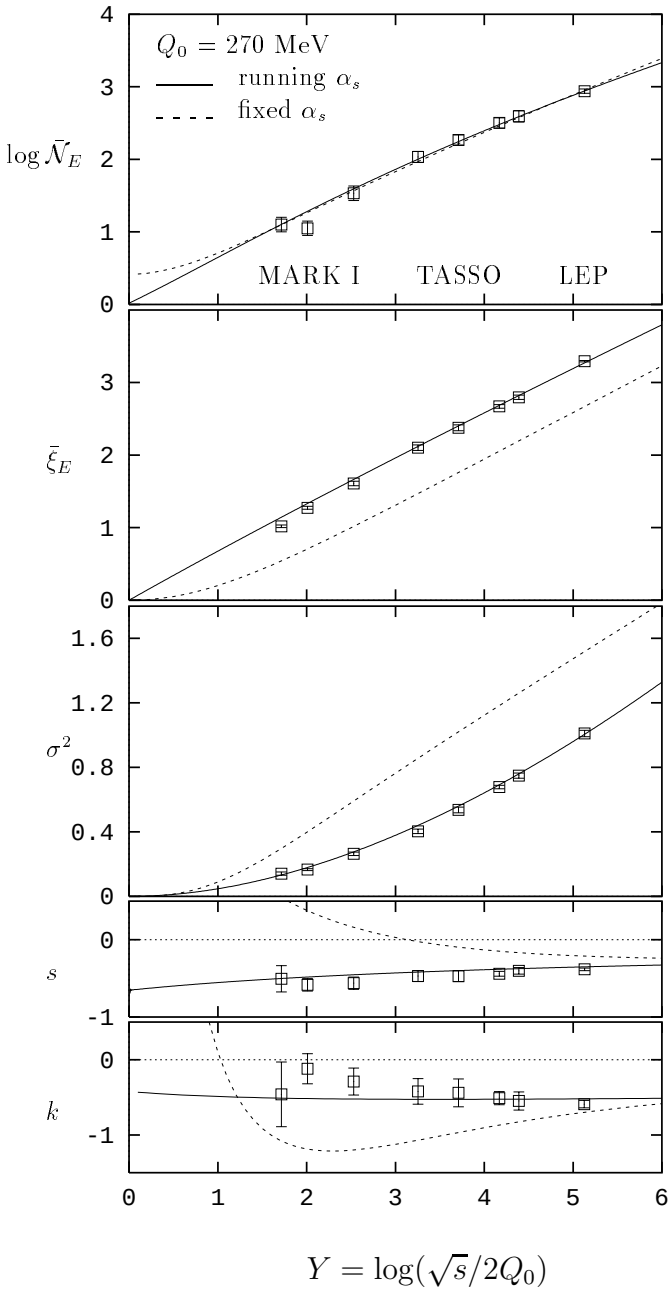

Fig. 1. The average multiplicity $\bar{\mathcal{N}}_E$ and the first four cumulants of charged particles' energy spectra Edn/dp vs. ξ_E,i.e., the average value $\bar{\xi}_E$, the dispersion σ^2, the skewness s and the kurtosis k, are shown as a function of $Y = \log(\sqrt{s}/2Q_0)$ for $Q_0 = 270$ MeV. Data points from MARK I[16] at $\sqrt{s} = 3$, 4.03, 7.4 GeV, TASSO[4] at $\sqrt{s} = 14$, 22, 35, 44 GeV and LEP at $\sqrt{s} = 91.2$ GeV (weighted averages of ALEPH[7], DELPHI[8], L3[6] and OPAL[5]). Predictions of the Limiting Spectrum (i.e. $Q_0 = \Lambda$) of MLLA with running α_s and of MLLA with fixed α_s are also shown (for $n_f = 3$). Predictions of the average multiplicity refer to the two-parameter formula $\bar{\mathcal{N}}_E = c_1 2^{\frac{4}{9}} \bar{\mathcal{N}}_{Part} + c_2$.

The predictions from MLLA with running α_s and normalization at threshold are remarkably successful considering the fact that there are only two parameters, actually coinciding, for the four cumulants. The deviation in $\bar{\xi}_E$ at the lower energies may suggest that the leading valence quark, which is now neglected by restricting to the D^+ spectrum, plays indeed a role at low c.m. energies. Otherwise, the predictions are confirmed at an almost quantitative level down to the lowest c.m. energies.

Figure 1 also shows the theoretical predictions for MLLA with fixed α_s (dashed lines) for the same value of Q_0 and n_f and $\gamma_0 = 0.64$. This value of γ_0 has been chosen in order to obtain a good fit for the average multiplicity, where we proceed as above to a fit with two additional free parameters. With this value of γ_0, the asymptotic slope for $\bar{\xi}_E$ is also well reproduced. An adjustement of the absolute normalization of $\bar{\xi}_E$ at a particular energy Y_0 would be possible if the perturbative QCD evolution towards lower energies and the normalization at threshold are abandoned. Looking at higher order moments, however, the model with fixed α_s is unable to reproduce the experimental behavior. In addition, the fixed α_s regime can be excluded already close to threshold. Indeed, if we suppose that the coupling is fixed for a certain energy interval near threshold $Y_0 \leq Y \leq Y_1$ and only runs for $Y > Y_1$, then $\bar{\xi}$ would be shifted towards smaller values because of the very different evolution near threshold, in contrast to the experimental behavior.

4.2. Rescaled cumulants

In addition to the standard moment analysis, it is interesting to consider the rescaled cumulants $\kappa_q/\bar{\xi}$; in the high energy limit they become energy independent in the model with fixed coupling (see eq. (10)) and therefore exhibit more directly the difference to the case of running coupling in the asymptotic domain.

Figure 2 show the experimental results on rescaled cumulants of order 2, 3 and 4 for $Q_0 = 270$ MeV; a clear Y-dependence in the available energy range is visible; this result is well reproduced by predictions of MLLA with running α_s and $n_f = 3$, while is again in contradiction with the constant behavior expected for fixed α_s. It would be interesting to continue this type of studies for instance at TEVATRON, where jets of higher energies are available, in order to test whether the rescaled cumulants show the remarkable dependence on Y predicted by the theory.

Let us also comment the dependence of the above results on the number of active flavors n_f. In leading order n_f enters only through the running coupling $\alpha_s(Y, n_f)$, while at next-to-leading level also through the parameter a. It has been argued that the number of flavors n_f should be kept fixed at 3, as light quarks should dominate quark-pair production in a well-developed cascade. However, one can also include heavy quark thresholds in the calculation simply by taking $\gamma_\omega(y)$ under the integral with n_f as the number of open flavors at energy y. Restricting our discussion to the leading term we note that in the original eq. (1) the scale of α_s is $k_t \simeq z(1-z)P < P/4$.

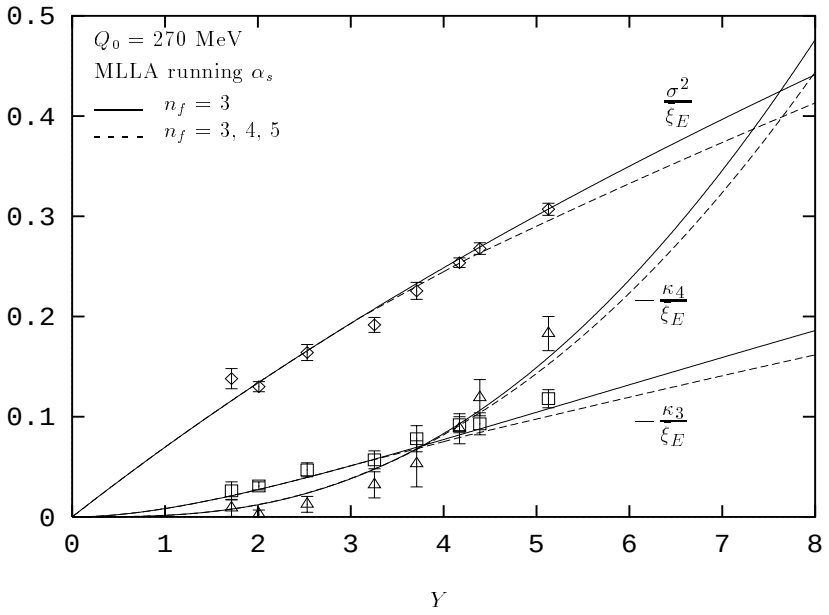

Fig. 2. Rescaled cumulants $\kappa_q/\bar{\xi}$ as a function of $Y = \log(\sqrt{s}/2Q_0)$ with the corresponding predictions of the Limiting Spectrum of MLLA with running α_s either without or with heavy flavors included. Data as in Figure 1. For fixed α_s these quantities approach constant values at high energies.

Therefore, we included the effect of heavy quarks in n_f for momentum $P > 4m_Q$. The effect of including heavy quarks thresholds in the model gives a correction of a few %, as shown for rescaled cumulants in Figure 2 (dashed lines). In addition, let us remind that further uncertainties on the scale of the running, two-loop effects and a possible explicit mass dependence of the coupling[17] are neglected in this approach.

4.3. Low-energy behavior: Boltzmann factor or running-α_s effect

Let us consider again the Lorentz-invariant distribution Edn/d^3p as a function of the particle energy E for small energies up to 1 GeV. The experimental exponential behavior is often related to the Boltzmann factor in the thermodynamical description of multiparticle production.

Figure 3a shows experimental data on the invariant distribution at three different c.m. energies. All three distributions tend to a common behavior at very low energies E, even though deviations from a simple exponential are visible at larger c.m. energies. Theoretical predictions for the Limiting Spectrum of MLLA with running α_s and for MLLA with fixed α_s (with $\gamma_0 = 0.64$) with the same value of Q_0 are also shown. Both theoretical curves are normalized to the experimental average multiplicity. Figure 3b compares the same data with theoretical predictions from the Limiting Spectrum of MLLA with running α_s in a wide energy range up to 30 GeV. It is remarkable that the Limiting Spectrum of MLLA is in good agreement with experimental data in a wide energy range and can approximately reproduced the exponential decrease of the spectrum in the low energy region. On the contrary,

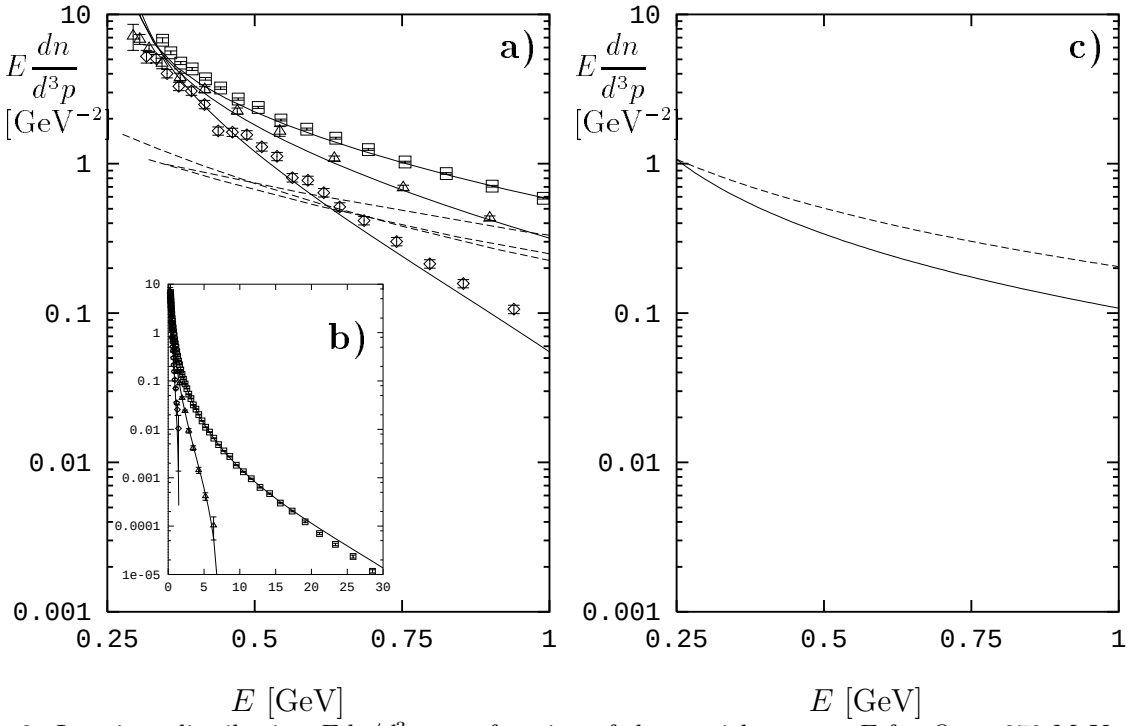

Fig. 3. Invariant distribution Edn/d^3p as a function of the particle energy E for $Q_0 = 270$ MeV. **a)** comparison of experimental data from MARK I[16] (diamonds), TASSO[4] (triangles) and OPAL[5] (squares) with predictions from MLLA with running α_s (Limiting Spectrum) (solid lines) and with fixed α_s (dashed lines). **b)** same as in **a)**, but in the energy range up to 30 GeV; only predictions from MLLA with running α_s are shown; **c)** analytical predictions of the Born term of DLA with running α_s (solid line) and with fixed α_s (dashed line); both curves are arbitrarily normalized to a common value.

the exact solution of the fixed-α_s model shows a flatter behavior, inconsistent with experimental behavior.

This behavior near the kinematical limit $E \to Q_0$ can be qualitatively understood in an analytical way in the DLA, where eq. (1) becomes:

$$D(\xi, y) = \delta(\xi) + \int_0^\xi d\xi' \int_0^y dy' \frac{C_a}{N_c} \gamma_0^2(y') D(\xi', y') \tag{15}$$

where $y = \log k\Theta/Q_0 = \log k_T/Q_0 = Y - \xi$.

The above evolution equation can be solved iteratively; with one iteration, one gets the Born term, which is the leading term in the limit $E \to Q_0$:

$$D(\xi, y) = \delta(\xi) + \frac{C_a}{N_c} \int_0^y dy' \gamma_0^2(y') \tag{16}$$

The difference between the fixed and the running α_s case is fully due to the expression of the anomalous dimension: in the fixed-α_s model, γ_0 becomes a constant, then:

$$D_{fix}(\xi, Y) = \delta(\xi) + \frac{C_a}{N_c} \gamma_0^2 (Y - \xi) \tag{17}$$

whereas for running α_s, $\gamma_0^2(y') = 12/b/(y' + \lambda)$,

$$D_{run}(\xi, Y) = \delta(\xi) + \frac{C_a}{N_c} \frac{12}{b} \log\left(\frac{Y - \xi + \lambda}{\lambda}\right) \tag{18}$$

Notice that in both cases the spectra go to finite values independent of c.m. energy in the limit $E \to Q_0$; the dependence of the spectrum on c.m. energy enters in higher orders terms. Predictions for the Born terms of DLA in the two models (with arbitrary normalization) are shown in Figure 3c; notice the relative enhancement at low energy E in the model with running α_s. This behavior can be intuitively explained: as for decreasing particle energy E also the typical particle p_t is necessarily decreasing, the coupling $\alpha_s(p_t/\Lambda)$ is rising in the running α_s case, whereas the fixed α_s model cannot account for such an effect.

5. Conclusions

The analysis of energy spectra in terms of moments has been performed. A consistent kinematical scheme to relate parton and hadron spectra in the low-energy region has been defined. This yields a good agreement of experimental data with theoretical predictions of MLLA with running α_s plus LPHD in a wide c.m. energy range from 3 GeV up to LEP energy. The best agreement with data is found for the Limiting Spectrum, where the two parameters of the theory coincide, i.e., $Q_0 = \Lambda$; the best value of Q_0 has been estimated to be 270±20 MeV. The zero-th order moment, i.e., the average multiplicity, requires two more parameters to fix the overall normalization for particle production and the leading particle contribution. Predictions of MLLA plus LPHD but with fixed coupling are inconsistent with the experimental behavior in the full energy range, thus showing a direct evidence for the running of the coupling in hadronic energy spectra. The effect of the running α_s is most pronounced near threshold where the variation of the coupling is strongest; it approximately reproduces the exponential dependence of the Lorentz-invariant distribution Edn/d^3p at low particle energies E of few hundreds MeV. The analysis of rescaled cumulants is shown to be more sensitive to the difference with the fixed-α_s regime in the high-energy region, for instance at TEVATRON energies. A similar analysis ranging from low to high values of the available energy can be performed also at HERA by looking at hadronic jet production in the Breit frame.

The obtained results give further support to the LPHD picture. A word of caution is appropriate nevertheless. The MLLA is based on high energy approximations (restriction to D^+ contribution, neglect of Next-to-Next-to-Leading effects) which have been extended into the low-energy region. A deviation in $\bar{\xi}$ at 3 GeV could indeed suggest that further contributions are needed. Also additional scheme-dependence of the coupling and two loop effects have been neglected in the calculation. Finally let us remind that we safely identified Q_0 with an effective hadron mass, since we referred to single inclusive spectra for all charged particles, but this identification cannot be pushed forward to single inclusive spectra for identified particles without taking into

account the effects of resonance decay, as recently shown in [18].

6. Acknowledgements

I am grateful to Wolfgang Ochs for fruitful suggestions on the content of this note. I would like to thank Ladislav Šandor and the Organizing Committee for the nice atmosphere created at this Symposium. Financial support from D.A.A.D. is gratefully acknowledged.

7. References

1. A. Bassetto, M. Ciafaloni, G. Marchesini, *Phys. Rep.* **100** (1983) 202
2. Yu.L. Dokshitzer, V.A. Khoze, A.H. Mueller, S.I. Troyan, *Rev. Mod. Phys.* **60** (1988) 373; *Basics of Perturbative QCD"*, Editions Frontières, Gif-sur-Yvette CEDEX-France (1991)
3. Yu. L. Dokshitzer, V. S. Fadin, V. A. Khoze, *Phys. Lett.* **B115** (1982) 242; *Z. Phys.* **C15** (1982) 325; A. Bassetto, M. Ciafaloni, G. Marchesini, A. H. Mueller, *Nucl. Phys.* **B207** (1982) 189; Ya. I. Azimov, Yu. L. Dokshitzer, V.A. Khoze, S.I. Troyan, *Z. Phys.* **C27** (1985) 65; *Z. Phys.* **C31** (1986) 213
4. TASSO Coll., W. Braunschweig et al., *Z. Phys.* **C47** (1990) 187
5. OPAL Coll., M. Z. Akrawy et al., *Phys. Lett.* **B247** (1990) 617
6. L3 Coll., B. Adeva et al., *Phys. Lett.* **B259** (1991) 199
7. ALEPH Coll., D. Buskulic et al., *Z. Phys.* **C55** (1992) 209
8. DELPHI Coll., P. Abreu et al., *Phys. Lett.* **B347** (1995) 447
9. ZEUS Coll., M. Derrick et al., *Z. Phys.* **C67** (1995) 93;
10. H1 Coll., S. Aid et al., *Nucl. Phys.* **B445** (1995) 3;
11. S. Lupia and W. Ochs, preprint MPI-PhT/95-86, September 1995, hep-ph/9509249; more details in paper eps0803 submitted to the "EPS-HEP 95", Brussels, 27.7-2.8.1995
12. C. P. Fong and B. R. Webber, *Nucl. Phys.* **B355** (1991) 54
13. Yu. L. Dokshitzer, V. A. Khoze and S. I. Troyan, *Int. J. Mod. Phys.* **A7** (1992) 1875
14. DASP Coll., R. Brandelik et al., *Phys. Lett.* **B67** (1977) 358
15. ADONE Coll., B. Esposito et al., *Lett. Nuovo Cimento* **19** (1977) 21
16. MARK I Coll., J. L. Siegrist et al., *Phys. Rev.* **D26** (1982) 969
17. Yu. L. Dokshitzer, D. V. Shirkov, *Z. Phys.* **C67** (1995) 449
18. DELPHI Coll., CERN preprint CERN-PPE/95-28, paper eps0539 submitted to the "EPS-HEP 95", Brussels, 27.7-2.8.1995